Rock Mechanics as a Multidisciplinary Science, Roegiers (ed.)
© 1991 Balkema, Rotterdam. ISBN 90 6191 194 X

Evaluation of optimal mud weight in soft shale levels

Ph.Charlez & O. Heugas
TOTAL-CFP, Scientific and Technical Center St Rémy Les Chevreuse, France

ABSTRACT : The main purpose of this paper is to present a model predicting mud density preventing from any mechanical instability when drilling wellbore in deep soft clay levels. To reach this goal, a classical Cam-Clay model is used as constitutive law in a finite element model coupled with a fluid diffusivity equation. The results show the strong dependency of stability on well deviation and time through a consolidation effect.
Material parameters are evaluated through oedometric and triaxial tests performed on cores and cuttings. Oedometric tests give very similar results while undrained triaxial tests display significant differences : closed form for cores and critical line for cuttings.

1 INTRODUCTION

80% of the wellbore problems are encountered when drilling soft shale or clay layers overlaying the payzone. For this type of rock, the origin of the problem can be chemical, mechanical or both.

On a chemical point of view, it is very well known that certain types of clay (particularly smectite) are strongly water sensitive [1,2] and tend to swell by hydratation when subjected to chemical gradients between the mud filtrate (water-based mud) and the water formation. This swelling phenomenon can be understood as an osmotic mechanism [3].

When the drilling fluid is an oil-based mud, wellbore instability has a purely mechanical origin. Its form depends on the rock rheology : either the material is "soft" and mainly controlled by large plastic strains and in that case, a "convergence" of the well towards its center will be observed, or the rock is more brittle and the mechanism known as "ovalization" will be very similar to that encountered in limestones or sandstones [4]. This paper is more particularly devoted to soft plastic clay materials. We exclude from the scope of this study hard brittle claystones. Nevertheless, we will see that this boundary between brittle an plastic shales is not so evident.

The only solution to prevent a well from mechanical instability is to contol the mud weight. The critical mud weight (preventing from any instability) will depend of course on the geostatic stresses, on the well diameter, on the deviation angle (generally high deviated wells will be more critical) but also on the material behaviour.

2 SPACE OF PARAMETERS

Let us consider a volume element submitted to a state of stress $\underset{\sim}{\sigma}$,a pore pressure p and undergoing a total strain increment $\underset{\sim}{d\epsilon}$. The strain energy associated with this transformation will be such that

$$dW = r d\epsilon + P dv \qquad (1)$$

with

$$P = \frac{1}{3}\sigma_{kk} - p \qquad dv = d\epsilon_{kk}$$

$$r = \sqrt{\frac{3}{2}(\underset{\sim}{s}:\underset{\sim}{s})} \qquad d\epsilon = \sqrt{\frac{2}{3}(\underset{\sim}{de}:\underset{\sim}{de})} \tag{2}$$

$$\underset{\sim}{s} = \underset{\sim}{\sigma} - \frac{1}{3}\sigma_{kk}\underset{\sim}{I} \qquad \underset{\sim}{de} = \underset{\sim}{d\epsilon} - \frac{1}{3}d\epsilon_{kk}\underset{\sim}{I}$$

Furthermore, as regards clay material, it is preferable to refer to void ratio e rather then porosity ϕ, the relationship between these parameters being :

$$e = \frac{\phi}{1-\phi} \tag{3}$$

If one neglects the compressibility of the matrix with respect to that of the pores, it can be demonstrated that the volumic strain only depends on the void ratio that is

$$dv = \frac{de}{1+e} \tag{4}$$

3 THE CAM-CLAY MODEL

The modified Cam-Clay model [5] is an elastoplastic isotropic associated constitutive law with a non linear elastic behaviour and a single contractant hardening mechanism. Furthermore, the matrix (i.e. grains) is supposed to be incompressible elastically and plastically.
We will content ourselves in this paper with a quick description of the model. More theoretical details can be found in [6].

3.1 State equation-Non linear elastic behaviour.

Let us consider a previously consolidated sample under a mean effective stress P_0 then completely unloaded, and given e_0 the void ratio in the unloaded state. If the sample is reloaded (slowly enough for the interstitial pressure to remain constant), it displays a non-linear elastic behaviour (Fig.1) with a slope κ known as "swelling coefficient" in the diagram e-lnP that is

$$e_e = e_0 - \kappa \ln P \tag{5}$$

3.2 Elastoplastic behaviour-Yield locus

One will assume the partitionning rule (small perturbations) between the elastic and the plastic void ratio increments that is

$$de = de_e + de_p \tag{6}$$

Furthermore, given the plastic incompressibility of the grains and assuming an associated plastic flow rule, the yield locus can be written using the effective plastic stress concept [7].
When $P = P_0$, plastic irreversibilities appear, the material hardens with a purely contractant mechanism and the plastic void ratio appears as a hardening variable in the process.
The yield locus characterizing this contractant plastic behaviour is written

$$f(P,r) = e_0 + e_p + (\lambda-\kappa)\ln\left[\frac{r^2+M^2P^2}{2M^2P}\right] - \Gamma = 0 \tag{7}$$

where κ, λ, M and Γ are material constants.

3.3 Plastic flow rule and hardening modulus

In the modified Cam-Clay model, the plastic potential is associated with the yield locus by the normality rule. The plastic flow rule is therefore written (the point indicates a derivative with respect to time)

$$\dot{v}_p = \lambda^* \frac{\partial f}{\partial P} \qquad \dot{\epsilon}_p = \lambda^* \frac{\partial f}{\partial r} \qquad \lambda^* = \frac{1}{H}\left[\frac{\partial f}{\partial r}dr + \frac{\partial f}{\partial P}dP\right] > 0 \qquad (8)$$

The plastic multiplier λ^* and the hardening modulus H can be calculated from the consistency condition

$$\frac{\partial f}{\partial P}\dot{P} + \frac{\partial f}{\partial r}\dot{r} + \frac{\partial f}{\partial e_p}\dot{e}_p = 0 \qquad (9)$$

Substituting (7) in (8) and (9),taking account of (4) and introducing the new variable $\eta = r/P$,one obtains

$$\dot{v}_p = -\frac{(\lambda-\kappa)}{(1+e)}\frac{\dot{P}}{P} + \frac{2\eta\dot{\eta}}{\eta^2+M^2} \qquad \dot{\epsilon}_p = \frac{\lambda-\kappa}{1+e}\left[\frac{2\eta}{M^2-\eta^2}\right]\left[\frac{2\eta\dot{\eta}}{\eta^2+M^2} + \frac{\dot{P}}{P}\right]$$

$$H = \frac{(1+e)\ (M^2-\eta^2)\ (\lambda-\kappa)}{P(\eta^2+M^2)} \qquad (10)$$

3.4 Physical signification of the material constants

a) Compressibility coefficient λ

Let us consider a purely hydrostatic test ($\eta = 0$).In that case,the first equation (10) is written

$$de_p = -(\lambda-\kappa)\frac{dP}{P} \qquad (11)$$

Differentiating (5) and taking account of (6),one obtains

$$de = -\lambda\frac{dP}{P} \qquad (12)$$

During hardening, the void ratio evolves like in the plastic domain with a logarithmic law (Fig.1) but with a slope λ known as "compressibility coefficient".

b) Critical state constant M

The expression of the hardening modulus shows that the r-P diagram can be divided into three domains corresponding respectively to $H>0$ ($\eta<M, \dot{v}_p<0$), $H=0$ ($\eta=M, \dot{v}_p=0$) and $H<0$ ($\eta>M, \dot{v}_p>0$).

These three zones can be easily understood if one considers the case of a triaxial test (Fig.2). If after consolidation under a mean effective stress P_0, the confining pressure σ_2 is maintained constant while the vertical load σ_1 is increased slowly under drained conditions (slope +3 in diagram r-P),the clay exhibits first a plastic contractant hardening ($H>0$) as described above,then an ideal plasticity phase($H=0$) during which the material strains at constant plastic volume and finally a rupture dilatant phase ($H<0$) known as "bifurcation" resulting in a localization of the deformations in a shear band. After this third phase, one can no longer strictly speak about rheological behaviour given the separation of the sample into two distinct structures.

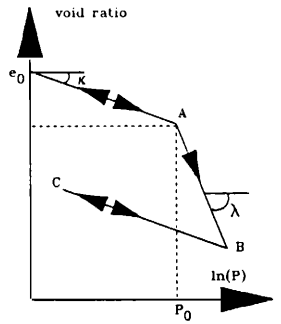

Fig.1.Behaviour of a clay under hydrostatic compression.

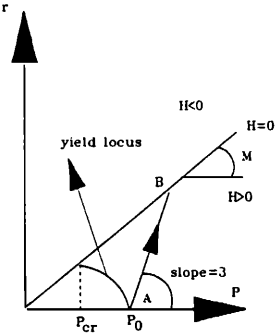

Fig. 2. Concept of critical state.

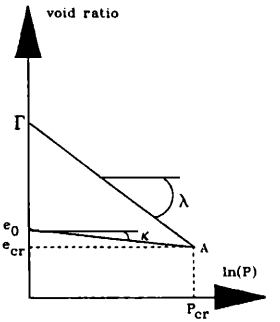

Fig. 3. Hardening law for the Cam-Clay.

The ideal plastic phase is known as "critical state". In diagram r-P it corresponds to a straight line r=MP. This critical line (which is not a yield locus) reflects in fact an internal friction mechanism without cohesion. Indeed,writing r=MP in the $\sigma_1 - \sigma_2$ diagram, one easily demonstrates that the associate Mohr-Coulomb friction angle equals $3M/(6+M)$.

c) Constant Γ

If the representative loading point is in the critical state (r=MP), the yield locus is written

$$e_{cr} = \Gamma - \lambda \ln P_{cr} \qquad (13)$$

Equation (13) illustrates that in the critical state, the void ratio e_{cr} and the mean effective stress P_{cr} are not independent. The constant Γ is equal to the critical void ratio for a critical mean effective stress equal to 1 bar (Fig.3).

The critical mean effective stress P_{cr} can be better understood if one assumes from point A first a complete elastic unloading that is

$$e_0 = e_{cr} + \kappa \ln P_{cr} \qquad (14)$$

then a new elastic reloading ($1 < P < P_{cr}$) such that

$$e = e_0 - \kappa \ln P \qquad (15)$$

Eliminating e_0 and e_{cr} from (13),(14),(15) one obtains

$$P_{cr} = \exp\left[\beta(e_0+e_p-\Gamma)\right] \qquad \beta = -\frac{1}{\lambda-\kappa} \qquad (16)$$

P_{cr} can be considered therefore as a hardening variable instead of e_p. Eliminating e_0+e_p from (7) and (16), the yield locus in the r-P plane, can be written as follows

$$f(P,r) = r^2 + M^2P^2 - 2\,M^2\,P\,P_{cr} = 0 \qquad (17)$$

which is the equation of ellipses in diagram r-P. If the critical mean effective stress increases according to (16), the yield locus enlarges (Fig.2) : the material hardens.

Let us note finally that P_{cr} is half the consolidation pressure. This can be easily verified since the consolidation pressure ($P=P_0$, $r=0$) belongs to the yield locus (17).

P_{cr}, P_0 or e_p can be therefore indifferently considered as hardening variables.

3.5 Parameters determination

The four parameters of the MCCM can be experimentally evaluated through oedometric and undrained triaxial tests

a) Oedometric test
An oedometric test is such that $d\epsilon_2=d\epsilon_3=0$. It corresponds to a stress path for which the ratio $K_0=(\sigma_h-p)/(\sigma_v-p)$ is a constant such that

$$K_0 = \frac{1}{2}\left[\frac{9}{3(1-\Lambda)+\sqrt{9\Lambda^2+4M^2}}\right] \quad -1 \text{ with } \Lambda = 1-\frac{\kappa}{\lambda} \qquad (18)$$

so that the mean effective stress is such that

$$P = \sigma'_v\left[\frac{1+2K_0}{3}\right] \qquad (19)$$

where σ'_v is the effective axial stress. During purely elastic and elastoplastic loadings,the slope will remain equal to κ and λ while the ordinate at origin e_η furnishes a relationship allowing determination of Γ provided M is known [6].

b) Undrained triaxial test
The shear resistance M can be evaluated through the deviatoric phase of a triaxial undrained test. Indeed one easily shows that during an undrained test (for which the void ratio remains constant since the grains are elastically and plastically incompressible), the mean effective stress evolves following the equation

$$P = \frac{P_0}{\left[1+\frac{\eta^2}{M^2}\right]^\Lambda} \qquad (20)$$

where P_0 is the initial consolidation mean effective stress.

Before the critical state is reached, the representative point moves towards point A until critical state at which it remains stable. Several undrained tests for different initial consolidation pressures allow therefore to determine M.

3.6 Fluid flow coupling

In the Cam-Clay, one assumes elastic and plastic incompressibility of the grains so that the plastic porosity (irreversible variation of porosity) is equal to the volumic plastic strain v_p. In these conditions it is easily demonstrated [6,7] that the hydraulic diffusivity equation only depends on the fluid properties that is

$$\frac{1}{K_f}\frac{\partial p}{\partial t} + \frac{1}{\phi}\frac{\partial v}{\partial t} = \frac{k}{\phi\mu}\nabla^2 p \qquad (21)$$

where K_f, k and μ are respectively the fluid compressibility, the rock permeability and the fluid viscosity.

4 EXAMPLE OF PARAMETERS DETERMINATION REPRESENTATIVITY OF REMOULDED SAMPLES

An example of parameters determination is now presented. The considered level is a deep Callovian clay (1800m) from "Bassin de Paris".

Generally core from these clay levels are not available since it does not correspond to the payzone. For this reason, the tests have to be performed with remoulded samples from cuttings.

Nevertheless to verify the representativity of the cuttings, a core has been taken in this same level and the parameters determination has been performed on both core and cuttings.

Results of oedometric tests are presented on Fig 4a for cuttings and Fig 4b for cores. The cuttings not being preconsolidated, the initial slope is equal to the compressibility coefficient λ, while for cores, a change of slope is observed since cores have been previously consolidated at the vertical effective in situ stress.

This effective vertical stress σ'_v is the difference between the weight of the overburden (obtained by integration of a density log) and the pore pressure. The latter will be assumed hydrostatic but this hypothesis will be verified further.

Under these hypotheses, one obtains at 1791m TVD

$$\sigma'_v = 411 \text{ bar} - 176 \text{ bar} = 235 \text{ bar}$$

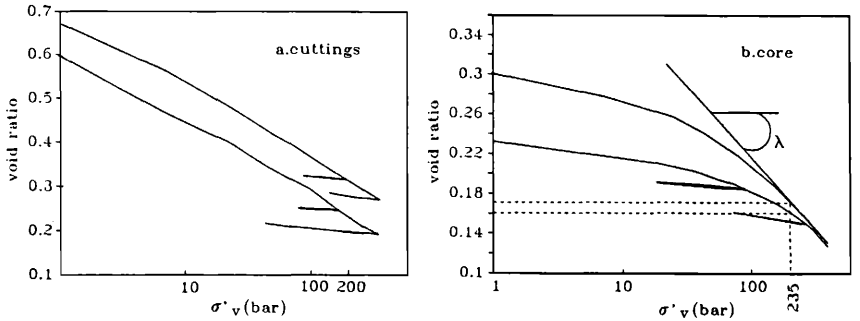

Fig. 4. Comparaison of oedometric tests between cuttings and core.

For cores, λ corresponds to the second slope (Fig 4b). Elastic unloading paths illustrate that swelling coefficients obtained from cuttings and cores are very close.

The results are summarized in the table below

Table I : results of oedometric tests on cuttings (remoulded samples) and cores

	λ	κ	$e(\sigma'_v)$
CUTTINGS	0.0756	0.0043	0.20
	0.0673	0.0074	0.29
	0.0886	0.0087	0.23
	0.0698	0.0090	0.22
	0.0766	0.0090	0.31
CORE	0.0769	0.0087	0.17
	0.0770	0.0055	0.16

The last column of Table I (void ratio corresponding to the vertical effective stress σ'_v) allows to calculate easily constant Γ and clearly shows that for a same effective stress, void ratio is generally higher for cuttings. This is mainly due to the fact that initial water content is higher for remoulded samples. The true value is of course that obtained from cores.

Critical state line (slope M) has been determined from four undrained triaxial tests at different confining pressures. Samples (core or cuttings) are firstly consolidated under a given confining pressure, then the axial load is slowly increased under undrained conditions until several percents of deformation.

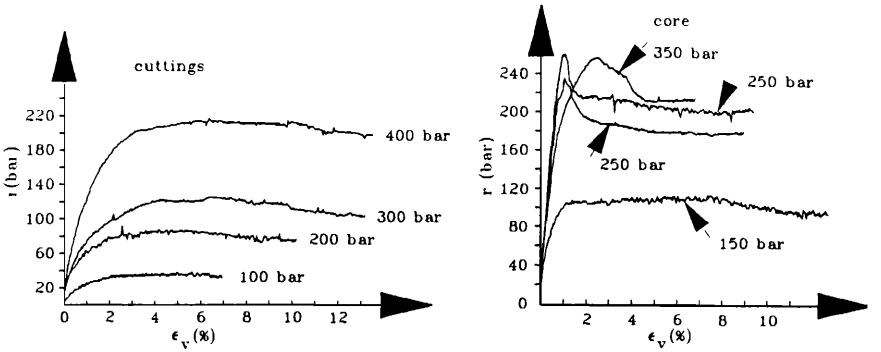

Fig. 5a. Comparaison of triaxial tests between cuttings and cores

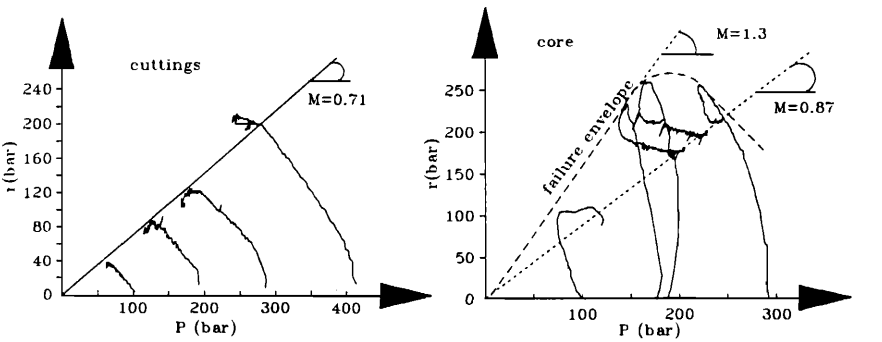

Fig. 5b. Comparaison of triaxial tests between cuttings and cores

For cuttings, the observed behaviour is very close to that described in the Cam-Clay model (Fig 5a) : after a positive strain hardening phase, a plateau is reached whose level (called undrained cohesion) depends on the consolidation effective stress. In r-P diagram, the observed curve (see eq 20) allows an easy determination of critical state slope (M = 0.71).

For cores, the behaviour is clearly different both in the r-ϵ_v and in the r-P diagrams (Fig 5b). Indeed, the tests exhibit a strong peak corresponding to a small amount of deformation (between 1 and 2 %). This peak illustrates the big difference between cuttings and core due to the presence of a true cohesion for the latter one. During the positive hardening phase, the strain energy is mainly stored into bounds between grains until the peak is reached. At this stage and during the subsequent softening-ideal plastic phase, the strain energy is released and the bounds break progressively leading to a material whose behaviour is very close to that of cuttings (relative irreversible movements of grains).

It is therefore not surprising that in the diagram r-P the initial failure envelope is not in very good accordance with a classical critical state line : with increasing confining pressure, the failure envelope closes like in porous chalk [8]. Nevertheless, we will define a mean initial pseudo critical line (Fig 5b) with a slope M = 1.30. During the softening-ideal plastic phase, this slope strongly decreases and the final points are very well aligned with a value of M = 0.87 (compare with M = 0.71 for cuttings).

5 APPLICATION TO WELLBORE STABILITY

The calculation of the critical mud weight avoiding any wellbore collapse is performed thanks to the 3D finite element model ISAM-GEO. The finite element mesh is presented on Fig 6. It contains 72 elements.

5.1 Boundary conditions

The vertical total stress σ_v is obtained by integration of a density log and as already mentioned leads to 411 bar at 1791m TVD.

Determination of initial pore pressure is one of the most difficult problem of such an approach. Generally one considers (comparing with payzone where pore pressure is well known) an "hydrostatic" value. This can be checked by comparing the in situ porosity issued from logs and the porosity deduced from the oedometric test at the same level. The in situ porosity can be derived from several logs (Neutron porosity, Formation Density Compensated, sonic). Due to the high clay content (60 %) several corrections are necessary and the true porosity is obtained through a treatment of these three logs. In the present case an average porosity of 13 % is computed. This porosity corresponds to a void ratio of 15 % which is close to the values $e(\sigma'_v)$ obtained on oedometric tests with core material (16 and 17 %). This means that the hypothesis of hydrostatic pressure is rather valid.

Finally, the effective horizontal stress is calculated from the vertical effective stress assuming an oedometric path that is (see eq 18)

$$\sigma'_h = K_0 \ \sigma'_v = 0.63 \times 235 \text{ bar} = 148 \text{ bar}$$

assuming $\lambda = 0.077$, $\kappa = 0.0071$ and $M = 1.30$.

5.2 Simulation of Drilling process

To simulate the drilling process in a stressed material, one applies first, at the wellbore boundary, nodal forces in equilibrium with the geostatic stresses. These nodal forces are then incrementally decreased which is equivalent to a decrease of the mud density. Two criteria are used to determine the critical mud weight : either one limits the convergence of the wellbore to a given value (between 3 % and 5 % of the initial wellbore diameter) or one chooses the smallest density for which no element is in the critical state.

Depending on the material properties (particularly κ and λ) one of these two criteria will be first verified.

These calculations are performed in undrained conditions. On the basis of the results of this undrained analysis, and for particular values of the mud weight, simulations are then realized at constant mud weight to appreciate the influence of pressure dissipation on stability (according to Eq 21).

6 RESULTS

The purpose of the present example is to evaluate the critical mud weight versus deviation for a 8 1/2" well.

The rock material being stiff the radial displacements remain small even for high deviations (less than 0.5 mm). The "ideal plasticity" criterion will be first verified and leads in undrained conditions to the following values for critical mud weight (critical state is reached when $Q/P = 1.3$) (Fig 7).

TABLE II : Critical mud weight versus deviation

MW	Deviation
1.46	80°
1.35	60°
<1.20	40° and 20°

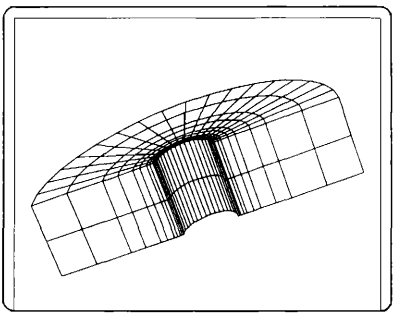

Fig. 6. Finite element mesh.

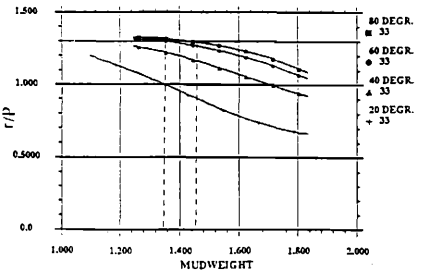

Fig.7. r/P versus mud weight for different well deviations (undrained conditions).

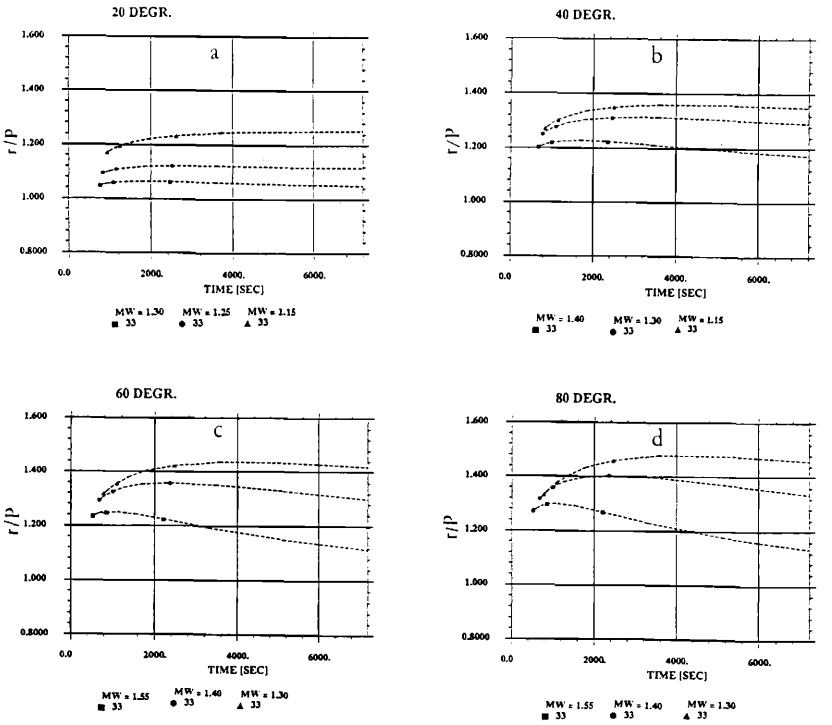

Fig. 8. Effect of consolidation on the ratio r/P for different well deviations.

The drainage effect is now studied (Fig 8a, b, c, d). For all deviations, pore pressure dissipation has a clear tendency to destabilize quickly the well (in spite of a low permeability, k = 0.12 μD). Critical mud weight has therefore to be increased and the final recommended values are summarized in Table III.

TABLE III : Critical mud weight versus deviation including pressure dissipation effect

MW	Deviation
1.54	80°
1.48	60°
1.31	40°
1.11	20°

7 CONCLUSIONS

Comparison between remoulded samples from cuttings and cores has clearly demonstrated that deep clay cannot be considered as cohesionless. While for cuttings the critical state concept (issued from Cam-Clay) remains valid, for cores, the failure envelope obtained from undrained triaxial tests appears as a closed form. On the contrary, oedometric tests give very similar results.

The Cam-Clay neglecting the cohesion, it can be considered as a "safety" constitutive law to appreciate wellbore stability. The presented example illustrates the great influence of well deviation on critical mud weight as well as time through a consolidation effect.

A more sophisticated constitutive law with several plastic mechanisms [9] should improve forecasts and should reduce the critical mud weight to a less safety value.

ACKNOWLEDGMENT : the authors thank TOTAL-CFP for allowing this paper to be published, ISAM-GBH for their help in the simulations and D. DESPAX for his advices.

REFERENCES :

[1] Denis, J.H. 1991. Compaction and Swelling of Ca-smectite in water and in $CaCl_2$ solutions. Submitted to Clay minerals

[2] Norrish, K. 1954. The swelling of montmorillonite : Disc. Faraday Soc. 18, 120-134

[3] Glueckauf, E. 1952. A theoretical treatment of cation exchangers. I: Proc. Roy. Soc. London A214, 207-225

[4] Guenot A. 1987. Contraintes et ruptures autour des forages pétroliers : 6th International Congress of Rock Mechanics - Montreal - Proc.pp109-118. Ed. Balkema

[5] Burland, I.B., Roscoe K.H., 1968, On the generalized stress strain behaviour of wet clay, in "Engineering Plasticity", Cambridge, Heyman-Leckie.

[6] Charlez, Ph. 1991 Rock Mechanics Vol I Theoretical fundamentals Ed. Technip in press.

[7] Coussy, O. 1991 Mécanique des milieux poreux Ed. Technip in press.

[8] Shao, J.F., Henry, J.P. and Guenot, A. 1988. An adaptative constitutive model for soft porous rocks (Chalk), Proc XXIXth U.S. Symposium, Minnesota, Mineapolis, Ed. Balkema.

[9] Lade, P.V., 1977. Elastoplastic stress strain theory for cohesionless soil curved yield surfaces, Int. J. Solid Structures, Vol 13, pp.1019-1036.